

# Positive braids of maximal signature

Autor(en): **Baader, Sebastian**

Objektyp: **Article**

Zeitschrift: **L'Enseignement Mathématique**

Band (Jahr): **59 (2013)**

PDF erstellt am: **12.07.2024**

Persistenter Link: <https://doi.org/10.5169/seals-515841>

## **Nutzungsbedingungen**

Die ETH-Bibliothek ist Anbieterin der digitalisierten Zeitschriften. Sie besitzt keine Urheberrechte an den Inhalten der Zeitschriften. Die Rechte liegen in der Regel bei den Herausgebern.

Die auf der Plattform e-periodica veröffentlichten Dokumente stehen für nicht-kommerzielle Zwecke in Lehre und Forschung sowie für die private Nutzung frei zur Verfügung. Einzelne Dateien oder Ausdrucke aus diesem Angebot können zusammen mit diesen Nutzungsbedingungen und den korrekten Herkunftsbezeichnungen weitergegeben werden.

Das Veröffentlichen von Bildern in Print- und Online-Publikationen ist nur mit vorheriger Genehmigung der Rechteinhaber erlaubt. Die systematische Speicherung von Teilen des elektronischen Angebots auf anderen Servern bedarf ebenfalls des schriftlichen Einverständnisses der Rechteinhaber.

## **Haftungsausschluss**

Alle Angaben erfolgen ohne Gewähr für Vollständigkeit oder Richtigkeit. Es wird keine Haftung übernommen für Schäden durch die Verwendung von Informationen aus diesem Online-Angebot oder durch das Fehlen von Informationen. Dies gilt auch für Inhalte Dritter, die über dieses Angebot zugänglich sind.

## POSITIVE BRAIDS OF MAXIMAL SIGNATURE

by Sebastian BAADER

ABSTRACT. We characterise positive braid links with positive Seifert form via a finite number of forbidden minors. From this we deduce a one-to-one correspondence between prime positive braid links of maximal signature and simply laced Dynkin diagrams, as well as a simple classification of alternating positive braid knots.

### 1. INTRODUCTION

A *positive braid link* is the closure of a positive braid, i.e. a finite product of the standard braid group generators  $\sigma_i$ . It is well known that positive braid links are fibred [7]; their fibre surface is the standard Seifert surface associated with the braid diagram and gives rise to a canonical Seifert form. The *signature*  $\sigma$  of a link is defined as the signature of the symmetrised Seifert form for any Seifert surface of the link. Positive braid links are known to have positive signature invariant [6]. The purpose of this paper is to classify positive braid links with maximal signature,  $\sigma = 2g$ , where  $g$  denotes the minimal genus of a link.

THEOREM 1. *There is a natural one-to-one correspondence between prime positive braids of maximal signature and simply laced Dynkin diagrams, reading as follows :*

$$\begin{array}{ll} A_n & \sigma_1^n \\ D_n & \sigma_1^n \sigma_2 \sigma_1^2 \sigma_2 \\ E_6 & \sigma_1^3 \sigma_2 \sigma_1^3 \sigma_2 \\ E_7 & \sigma_1^4 \sigma_2 \sigma_1^3 \sigma_2 \\ E_8 & \sigma_1^5 \sigma_2 \sigma_1^3 \sigma_2 \end{array}$$

*Naturality* means that the quadratic form associated with the Dynkin diagrams is isomorphic to the symmetrised Seifert form of the corresponding braids. The knots arising from the series  $A_n$  and  $E_6, E_8$  are the torus knots of type  $T(2, n)$  ( $n \in \mathbf{N}$  odd),  $T(3, 4)$  and  $T(3, 5)$ , respectively. The other diagrams give rise to links with two or three components.

The proof of Theorem 1 is based on a version of minor theory for Seifert surfaces, inspired by graph minor theory [3]. We define a *minor of a Seifert surface* as a subsurface that induces an inclusion on the level of first homology groups, i.e. a subsurface all of whose complementary components are adjacent to the boundary of the surrounding surface. The minor relation for Seifert surfaces is designed to preserve positivity of the Seifert form. In the case of positive braids, we will characterise positivity of the Seifert form via four forbidden minors.

**THEOREM 2.** *Let  $L \subset \mathbf{R}^3$  be a positive braid link with non-positive Seifert form. Then the fibre surface of  $L$  contains a minor of type  $T, E, X$  or  $Y$ .*

Here the surfaces of type  $T, E, X$  and  $Y$  are the canonical fibre surfaces of the positive braids  $\sigma_1^4 \sigma_2 \sigma_1^4 \sigma_2$ ,  $\sigma_1^6 \sigma_2 \sigma_1^3 \sigma_2$ ,  $\sigma_1 \sigma_2^2 \sigma_1 \sigma_3 \sigma_2^2 \sigma_3$  and  $\sigma_1^3 \sigma_2^2 \sigma_1^3 \sigma_2$ , respectively. The meaning of these will shortly become clear.

We conclude the introduction with a remarkable consequence of Theorem 1. Let  $L$  be a prime alternating positive braid knot. According to Rasmussen [5], we have two equalities,  $\sigma = s = 2g$ , between the signature  $\sigma$ , the Rasmussen invariant  $s$  and twice the minimal genus  $g$  of  $L$ . In particular, the link  $L$  has maximal signature. We are left with  $T(2, n)$ ,  $T(3, 4)$  and  $T(3, 5)$  as potential prime alternating positive braid knots. The latter two are non-alternating.

**COROLLARY 3.** *The torus knots of type  $T(2, n)$  are the only prime alternating positive braid knots.*

According to Cromwell [2], the prime components of a positive braid link are positive braid links. Therefore, alternating positive braid knots are connected sums of torus knots of type  $T(2, n)$ . This statement fits well with the following result due to Nakamura [4] and Stoimenow [8]: positive alternating links have positive alternating diagrams.

**ACKNOWLEDGEMENTS.** I would like to thank David Cimasoni for numerous valuable suggestions, clarifying the notion of a surface minor and for his help in setting up the organisation of this manuscript.

2. BRICK DIAGRAMS AND LINKING TREES

The fibre surface of a positive braid link consists of vertical discs, one for each string, and horizontal bands, one for each crossing. It naturally retracts on a graph with vertical and horizontal edges called *brick diagram*. We will use brick diagrams as a notation for positive braids, as well as their fibre surfaces. Brick diagrams for the braids appearing in Theorems 1 and 2 are depicted in Figure 1.

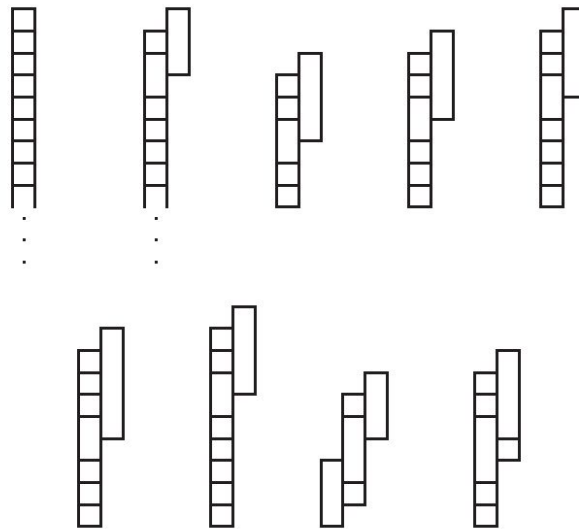


FIGURE 1

Brick diagrams for  $A_n$ ,  $D_n$ ,  $E_6$ ,  $E_7$ ,  $E_8$  and  $T$ ,  $E$ ,  $X$ ,  $Y$

The rectangles of a brick diagram (with the positive orientation) can be thought of as a basis for the first homology group of the fibre surface. In particular, deleting a horizontal or vertical edge of a brick diagram gives rise to a minor surface. We will use this fact throughout the paper. The symmetrised Seifert matrix with respect to the rectangle basis is easy to determine from a brick diagram. All its diagonal entries are 2; the remaining coefficients are 1 or 0, depending on whether the corresponding pairs of rectangles are linked or not. Here two rectangles are *linked*, if and only if they are arranged as in the braids  $\sigma_1^3$ ,  $\sigma_1\sigma_2\sigma_1\sigma_2$  or  $\sigma_2\sigma_1\sigma_2\sigma_1$ . Indeed, these all represent the positive trefoil knot. The rectangles of the braid  $\sigma_1\sigma_2\sigma_2\sigma_1$  are not linked, since this represents a connected sum of two positive Hopf links. In the above examples, the rectangles are linked in a tree-like pattern (see Figure 2).

The resulting symmetrised Seifert matrices are nothing but the Cartan matrices of the linking trees, viewed as Coxeter systems. The first five are

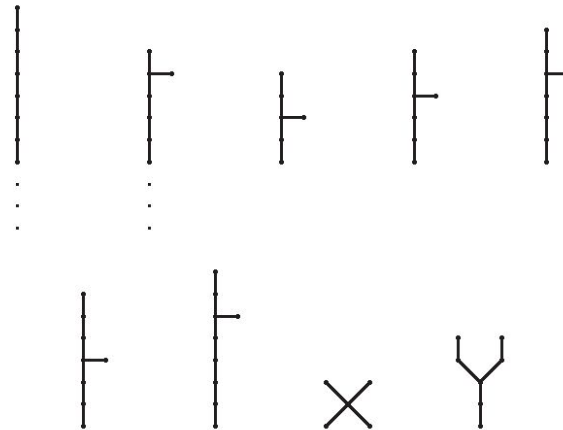


FIGURE 2  
Linking trees for  $A_n, D_n, E_6, E_7, E_8$  and  $T, E, X, Y$

positive definite since they correspond to spherical Coxeter systems. The remaining four matrices are

$$\begin{pmatrix} 2 & 1 & 1 & 0 & 0 & 1 & 0 & 0 \\ 1 & 2 & 0 & 0 & 0 & 0 & 0 & 0 \\ 1 & 0 & 2 & 1 & 0 & 0 & 0 & 0 \\ 0 & 0 & 1 & 2 & 1 & 0 & 0 & 0 \\ 0 & 0 & 0 & 1 & 2 & 0 & 0 & 0 \\ 1 & 0 & 0 & 0 & 0 & 2 & 1 & 0 \\ 0 & 0 & 0 & 0 & 0 & 1 & 2 & 1 \\ 0 & 0 & 0 & 0 & 0 & 0 & 1 & 2 \end{pmatrix}, \begin{pmatrix} 2 & 1 & 1 & 0 & 1 & 0 & 0 & 0 & 0 \\ 1 & 2 & 0 & 0 & 0 & 0 & 0 & 0 & 0 \\ 1 & 0 & 2 & 1 & 0 & 0 & 0 & 0 & 0 \\ 0 & 0 & 1 & 2 & 0 & 0 & 0 & 0 & 0 \\ 1 & 0 & 0 & 0 & 2 & 1 & 0 & 0 & 0 \\ 0 & 0 & 0 & 0 & 1 & 2 & 1 & 0 & 0 \\ 0 & 0 & 0 & 0 & 0 & 1 & 2 & 1 & 0 \\ 0 & 0 & 0 & 0 & 0 & 0 & 1 & 2 & 1 \\ 0 & 0 & 0 & 0 & 0 & 0 & 0 & 1 & 2 \end{pmatrix},$$

$$\begin{pmatrix} 2 & 1 & 1 & 1 & 1 \\ 1 & 2 & 0 & 0 & 0 \\ 1 & 0 & 2 & 0 & 0 \\ 1 & 0 & 0 & 2 & 0 \\ 1 & 0 & 0 & 0 & 2 \end{pmatrix}, \begin{pmatrix} 2 & 1 & 0 & 1 & 0 & 1 & 0 \\ 1 & 2 & 1 & 0 & 0 & 0 & 0 \\ 0 & 1 & 2 & 0 & 0 & 0 & 0 \\ 1 & 0 & 0 & 2 & 1 & 0 & 0 \\ 0 & 0 & 0 & 1 & 2 & 0 & 0 \\ 1 & 0 & 0 & 0 & 0 & 2 & 1 \\ 0 & 0 & 0 & 0 & 0 & 1 & 2 \end{pmatrix}$$

and have determinant zero<sup>1)</sup>. As a consequence, every Seifert surface that contains one of the surfaces  $T, E, X, Y$  as a minor has non-positive Seifert form. We will prove the converse in the next section.

<sup>1)</sup> Incidentally, these correspond to the simply laced affine Coxeter systems (see [1] for an elegant characterisation of spherical and affine Coxeter systems).

3. PROOFS OF THEOREMS 1 AND 2

In this section, we will prove the following two statements, which together imply Theorems 1 and 2.

- (1) A braid link represented by a prime positive 3-braid either corresponds to a simply laced Dynkin diagram, or contains one of the minors  $T, E, X, Y$ .
- (2) The fibre surface of a prime positive braid with at least 4 strings contains a minor of type  $X$ .

The cases of 3-braids and 4-braids require special care.

3-BRAIDS

Let  $L$  be a link represented by a positive 3-braid  $\beta$ . Applying the braid relation  $\sigma_2\sigma_1\sigma_2 = \sigma_1\sigma_2\sigma_1$  and conjugation to  $\beta$  does not affect the link type of its closure. Therefore, we may assume that

$$\beta = \sigma_1^{a_1} \sigma_2^{b_1} \sigma_1^{a_2} \sigma_2^{b_2} \dots \sigma_1^{a_m} \sigma_2^{b_m}$$

with all  $a_i \geq 2, b_k \geq 1$ . We use

$$(a_1, \underbrace{0, \dots, 0}_{b_1-1}, a_2, \underbrace{0, \dots, 0}_{b_2-1}, a_3, \dots, a_m, \underbrace{0, \dots, 0}_{b_m-1})$$

as a shortcut for  $\beta$ . In this notation the braids of the forbidden minors  $T, E, Y$  read  $(4, 4), (6, 3)$  and  $(3, 0, 3)$  (see again Figure 1). The surface  $X$  cannot be defined by a 3-braid. Nevertheless, it is a minor of the fibre surface of the 3-braid  $(2, 0, 2, 0)$ , as shown in Figure 3. Note that the second brick diagram represents a Seifert surface in a straightforward way, but not a braid. Here and thereafter equality between brick diagrams means isotopy of surfaces or, equivalently, of their boundary links. The latter is easy to verify. We distinguish four types of braids  $\beta$  depending on the number  $m \in \mathbf{N}$ .



FIGURE 3

If  $m \geq 4$  then the braid  $\beta$  (more precisely its fibre surface) contains  $(2, 2, 2, 2)$  as a minor, by cutting a suitable number of crossings. After deleting two more crossings of type  $\sigma_2$ , we end up with  $(4, 4)$ , the forbidden minor  $T$ .

If  $m = 3$  and at least one  $b_k \geq 2$  then  $\beta$  contains  $(2, 2, 2, 0)$ , hence  $(2, 0, 2, 0)$ , in turn the forbidden minor  $X$ .

If  $m = 3$  and all  $b_k = 1$  then either  $\beta$  is one of  $(2, 2, 2)$ ,  $(2, 2, 3)$  or  $\beta$  contains one of  $(2, 3, 3)$ ,  $(2, 2, 4)$ . The closures of the first two braids are easily identified as  $E_7$  and  $E_8$ . The others contain the forbidden minors  $(3, 0, 3)$  and  $(4, 4)$ , i.e.  $Y$  and  $T$ .

If  $m = 2$  and both  $b_k \geq 2$  then  $\beta$  contains  $(2, 0, 2, 0)$ , in turn  $X$ .

If  $m = 2$  and one  $b_k \geq 2$  then either  $\beta$  contains the forbidden minor  $(3, 0, 3)$  or  $\beta = (2, a, \underbrace{0 \dots 0}_{b-1})$ , which represents the same link as  $(a, b + 1)$ .

This is illustrated in Figure 4, for  $a = 4$ ,  $b = 5$ .

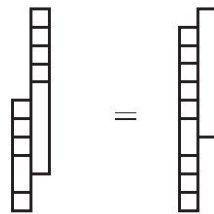


FIGURE 4

If  $m = 2$  and both  $b_k = 1$  then either  $\beta$  contains one of the forbidden minors  $(6, 3)$ ,  $(4, 4)$  or  $\beta$  is one of  $(n, 2)$ ,  $(3, 3)$ ,  $(4, 3)$ ,  $(5, 3)$ . These are the braids of type  $D_n$ ,  $E_6$ ,  $E_7$  and  $E_8$ .

If  $m = 1$  then  $\beta$  represents a torus link with 2 strings (type  $A_n$ ) or a connected sum of two such links.

4-BRAIDS

Let  $L$  be a link represented by a positive 4-braid  $\beta$ . We suppose that  $\beta$  is *irreducible* and *minimal*, i.e.  $\beta$  does not decompose into a connected sum of two non-trivial positive braids and  $\beta$  has the least braid index among all positive braids representing  $L$ . Contrary to above, we suppose that  $\beta$  has no subwords of the form  $\sigma_1\sigma_2\sigma_1$  and  $\sigma_2\sigma_3\sigma_2$ . From this and irreducibility we deduce that  $\beta$  contains the fibre surface of the braid  $\sigma_2^2\sigma_1\sigma_2^2\sigma_1$  as a minor. In addition,  $\beta$  contains at least two non-consecutive generators  $\sigma_3$ . Keeping in mind that there is no subword of the form  $\sigma_2\sigma_3\sigma_2$ , we are left with one of the four minors shown in Figure 5.

The first three contain  $X$  as a minor (for the third one, this is best seen after the deformation shown in the figure). The last one can be reduced to a

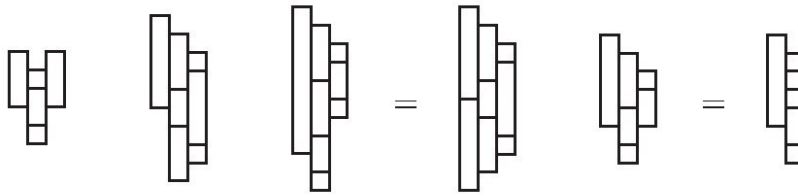


FIGURE 5

3-braid and does not contain  $X$  as a minor. In that case  $\beta$  must have at least one more crossing of type  $\sigma_2$  or  $\sigma_3$  in order to be a minimal braid. A careful examination brings up two more minors containing  $X$ , see Figure 6.

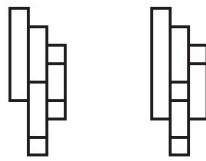


FIGURE 6

$n$ -BRAIDS ( $n \geq 5$ )

Let  $L$  be a link represented by a positive, irreducible and minimal  $n$ -braid  $\beta$  ( $n \geq 5$ ). As in the case of 4-braids, we may suppose that  $\beta$  contains a minor of the form  $\sigma_2^2\sigma_1\sigma_2^2\sigma_1$ , as well as a symmetric version thereof on the right,  $\sigma_{n-2}^2\sigma_{n-1}\sigma_{n-2}^2\sigma_{n-1}$ . Since  $\beta$  is irreducible, there exists a chain of small rectangles, successively linked, connecting a rectangle in the second column to a rectangle in the second to last column, as illustrated in Figure 7. The resulting surface manifestly contains  $X$  as a minor.

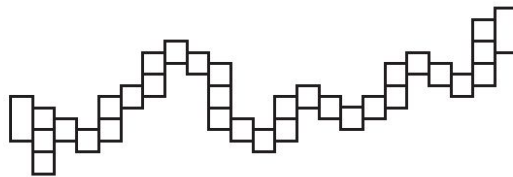


FIGURE 7

In summary, prime positive braid links of minimal braid index  $n \geq 4$  have non-positive Seifert form. Non-positivity of the Seifert form is detected by four forbidden minors  $T, E, X, Y$ . At last, every prime positive braid link with positive Seifert form corresponds to a simply laced Dynkin diagram. This concludes the proof of Theorems 1 and 2.



It is conceivable that Theorem 2 carries over to larger classes of fibre surfaces, as long as they share certain features with positive braid surfaces. More explicitly, we may ask whether Theorem 2 holds for all fibre surfaces supporting the tight contact structure on  $S^3$ .

## REFERENCES

- [1] A'CAMPO, N. Sur les valeurs propres de la transformation de Coxeter. *Invent. Math.* 33 (1976), 61–67.
- [2] CROMWELL, P.R. Positive braids are visually prime. *Proc. London Math. Soc.* (3) 67 (1993), 384–424.
- [3] LOVÁSZ, L. Graph minor theory. *Bull. Amer. Math. Soc. (N.S.)* 43 (2006), 75–86.
- [4] NAKAMURA, T. Positive alternating links are positively alternating. *J. Knot Theory Ramifications* 9 (2000), 107–112.
- [5] RASMUSSEN, J. Khovanov homology and the slice genus. *Invent. Math.* 182 (2010), 419–447.
- [6] RUDOLPH, L. Nontrivial positive braids have positive signature. *Topology* 21 (1982), 325–327.
- [7] STALLINGS, J. Constructions of fibred knots and links. In: *Algebraic and Geometric Topology*, 55–60. Proc. Sympos. Pure Math. 32. Amer. Math. Soc., Providence, R.I., 1978.
- [8] STOIMENOW, A. On some restrictions to the values of the Jones polynomial. *Indiana Univ. Math. J.* 54 (2005), 557–574.

(Reçu le 4 mars 2013)

Sebastian Baader

Universität Bern  
Sidlerstrasse 5  
CH-3012 Bern  
Switzerland  
*e-mail* : sebastian.baader@math.unibe.ch